Application of Raman Lidar to Air Quality Measurements

C. Russell Philbrick and Karoline R. Mulik
Penn State University
Department of Electrical Engineering
University Park PA 16802

ABSTRACT

Raman lidar techniques have been demonstrated which provide most valuable descriptions of the evolution of air pollution events. The vibrational and rotational Raman lidar signals provide simultaneous profiles of meteorological data, ozone and measurements of airborne particulate matter. An operational prototype Raman lidar instrument was prepared and demonstrated for the US Navy and is now used for scientific investigations. It makes use of 2nd and 4th harmonic generated laser beams of a Nd:YAG laser to provide both daytime and nighttime measurements. The Raman scatter signals from vibrational states of water vapor and nitrogen provide robust profiles of the specific humidity in the lower atmosphere. The temperature profiles are measured using the ratio of rotational Raman signals at 530 and 528 nm from the 532 nm (2nd harmonic) beam of the Nd:YAG laser. In addition, the optical extinction profiles are determined from the measured gradients in each of several molecular profiles compared to the molecular scale height. We currently use the wavelengths at 284 nm (nitrogen vibrational Raman), 530 nm (rotational Raman) and 607 nm (nitrogen vibrational Raman) to determine profiles of optical extinction. The ozone profiles in the lower troposphere are measured using a DIAL analysis of the ratio of the vibrational Raman signals for nitrogen (284 nm) and oxygen (278 nm), which are on the steep side of the Hartley band of ozone. Several data sets have been obtained during air pollution events and the results from these events have been the subject of recent studies. The examples presented in this paper have been selected to show the new level of understanding of air pollution events that is being gained from applications of lidar techniques.

Keywords: Raman scatter, lidar remote sensing, air pollution, optical extinction, tropospheric ozone

1. INTRODUCTION

During the last decade, there has developed a rising concern for the influence that man's activity has upon the environment of our planet. No longer can we view the atmosphere, ocean and land mass as sufficiently large and resilient to withstand the abuses of careless waste and pollution. In particular, the atmosphere has shown changes that have been demonstrated to affect personal health, influence our activities due to optical visibility changes, and cause concern for stability of our global environment due to "greenhouse effects." The two principal components of the atmosphere that have been singled out as major concerns of air pollution are ozone and airborne particulate matter (PM). Ozone is a known toxic species that causes deleterious respiratory effects, particularly causing blisters in the respiratory tract, ageing of tissue and complications for older individuals and those with asthma and other respiratory problems.[1,2] The increase in air borne particulate matter has changed the optical properties of the atmosphere by decreasing visibility which directly affects air traffic patterns and landing frequency of commercial aircraft, and by reducing the aesthetic appreciation of our national parks.[3] The increase of emissions into the atmosphere causes two competing mechanisms which affect the energy balance that controls our global climate. The increase in emission of chemical species into the atmosphere that absorb infrared radiation lead to global warming due to the greenhouse effect. It is certainly true that the CO_2 has been increased by the burning of fossil fuels. On the other hand, increasing airborne particulate matter reduces the direct and indirect flux of solar radiation at the surface by cloud formation and changes in the planetary albedo. Increases in optical scattering caused by airborne particulate matter could result in reduction of global temperature, thus counteracting the increases expected from the greenhouse effect. The increase in airborne particulate matter is principally due to combustion products associated with transportation and power generation.[2] The goal of present research is to assist in understanding the details of the physical and chemical processes that result in air pollution episodes and global environment changes, so that logical policies can be developed that will avert sever situations and show the best directions for action. The Raman lidar described here is proposed as an important tool for gaining that understanding.

In *Laser Radar Technology and Applications V*, Gary W. Kamerman, Upendra N. Singh, Christian Werner, Vasyl V. Molebny, Editors, Proceedings of SPIE Vol. 4035 (2000) • 0277-786X/00/$15.00

The Raman lidar provides a robust tool that can be employed to measure a wide range of meteorological and environmental properties.[4] The most important parameters for testing our understanding by comparison with air pollution model calculations are ozone and particulate matter. In the past, the general approach used to developing the data base for this evaluation has been based upon networks of ground sites that make local *insitu* measurements. Prior investigations have suffered from the fact that little information on the vertical structure was available because of the expense of using aircraft and balloon platforms to obtain measurements aloft. The Raman lidar can provide continuous time sequences of the vertical profiles of the key parameters in the lower atmosphere. The examples of profiles shown here demonstrate the capability for measuring the needed properties. The ozone profiles in the lower atmosphere are measured directly from the absorption in the Hartley band. The particulate mater is determined from the measurements of optical extinction and backscatter at visible and ultraviolet wavelengths. The most important meteorological parameters are temperature and water vapor. Temperature is measured from the distribution of the scattered rotational Raman intensity. The water vapor is determined from the specific humidity measured by the ratio of the vibrational Raman radiation scattered by water vapor and molecular nitrogen. The water vapor is a particularly important tracer of the tropospheric dynamics and is the best marker of the thickness of the planetary boundary layer. The Raman lidar techniques used to investigate air pollution events will be described in the following section. Examples from the results of several investigations will be shown as examples of the capability of Raman lidar to be used as a tool for studies of the physical and chemical processes active during air pollution events.

2. RAMAN LIDAR MEASUREMENT TECHNIQUES

Raman scattering is one of the processes that occurs when optical radiation is scattered from the molecules of the atmosphere. It is most useful because the vibrational Raman scattering provides distinct wavelength shifts for species specific vibrational energy states of the molecules and rotational Raman scattering provides a signal with a wavelength shift that depends directly upon the atmospheric temperature.[4] Figure 1(a) shows a diagram of the vibrational and rotational energy levels that are associated with Raman scatter. When a photon scatters from a molecule, the redistribution of the charge cloud results in a virtual energy state. Most of the atmospheric molecules reside in the ground vibrational level because the vibrational excitation corresponds to relatively large energy transitions (tenths of eV) for simple molecules like nitrogen and oxygen compared to the thermal energy available. After the scattering occurs, most of the events result in the return of the molecule to the ground state and the emitted photon has the energy of the initial photon plus/minus the random thermal velocity of the molecule, that is the Doppler broadening. A small fraction of the transitions (order of 0.1%) result in giving part of the photon energy to the molecule, and ending in the first vibrational level (a Stokes transition). The emitted photon energy is decreased by exactly the energy of the vibrational quanta for that molecule. For the small fraction of molecules existing in the vibrational excited level, the unlikely anti-Stokes transition is possible and results in a photon with energy increased by the vibrational state increment. The relative sensitivity of the scattering from the vibrational and rotational states is indicated by the scattering cross-section values for scattering by a frequency doubled Nd:YAG laser at 532 nm shown in Figure 1(b). The wavelengths of vibrational Raman back scatter signals from the molecules of the water vapor and molecular nitrogen are widely separated from the exciting laser radiation and can be easily isolated for measurement using modern filter technology and sensitive photon counting detectors.[5] The ratio of rotational Raman signals at 528 nm and 530 nm provides a measurement which is sensitive to atmospheric temperature.[6,7] All of the molecules of the lower atmosphere are distributed in the rotational states according the temperature. By measuring the ratio scattered signals at two wavelengths in this distribution, the temperature can be directly measured. In order to push the lidar measurement capability into the daylight conditions, we have used the "solar blind" region of the spectrum between 260 and 300 nm. The "solar blind" region is darkened by the stratospheric ozone absorption of ultraviolet radiation, however care must be given to account for the interference of tropospheric ozone absorption in this region. Night time measurements are made using the 660nm/607nm (H_2O/N_2) signal ratio from the doubled Nd:YAG laser radiation at 532 nm. Daylight measurements are obtained using the 295nm/284nm (H_2O/N_2) ratio from the quadruple Nd:YAG laser radiation at 266 nm. A small correction for the tropospheric ozone must be applied. That correction can be obtained from the ratio of the O_2/N_2 signals 278nm/284nm, and from this analysis the ozone profile in the lower troposphere is also obtained.[8] The Raman techniques, which use of ratios of the signals for measurements of water vapor and temperature, have the major advantage of removing essentially all of uncertainties, such as any requirement for knowledge of the absolute sensitivity and non-linear factors caused by aerosol and cloud scattering.[9] Optical extinction is measured using the gradient of the measured molecular profile compared with that expected for the density gradient. Since the Raman signal is only scattered from the molecular component of the scattering volume, and difference in the gradient of the signal from that expected due to loss from molecular scattering and absorption can be used to calculate the aerosol extinction.[10-14]

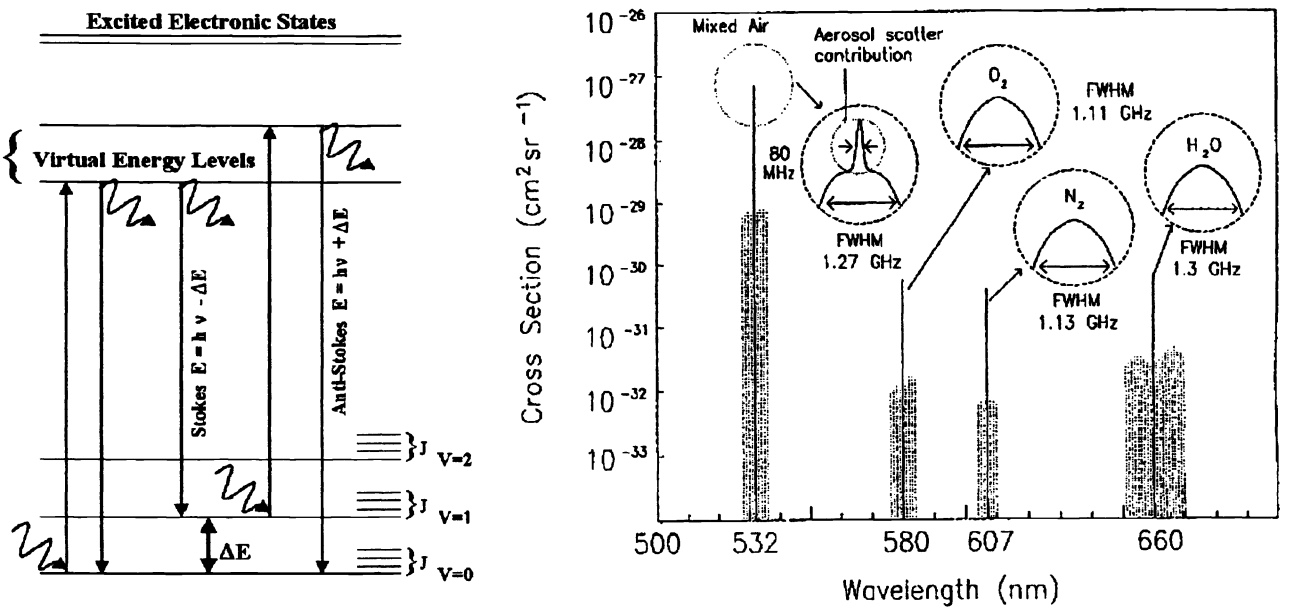

(a) (b)

Figure 1. (a) The energy diagram of a molecule illustrates that the scattering of a photon raises the molecule to a virtual level which normally decays to ground (V=0) emitting a photon of the same energy as the incident energy, only broadened by thermal Doppler velocity. In a small fraction of cases, the return is Raman shifted to the first vibrational level (V=1), a Stokes shift. The relatively large vibrational energy (ΔE) compared with thermal energy makes the Anti-Stokes vibrational transition unlikely, however, the rotational states (J-levels) are populated by thermal excitation, (b) The relative intensities of the Stokes vibrational Raman shifts of oxygen, nitrogen and water vapor are indicated for illumination of atmospheric molecules with the 532 nm laser. The expected line widths and the relative rotational states are indicated.[4]

2.1. Lidar Equation

The power of the signal measured by a monostatic lidar system is described by,

$$(\lambda_R, z) = E_T(\lambda_T)\,\xi_T(\lambda_T)\,\xi_R(\lambda_R)\,\frac{c\tau}{2}\,\frac{A}{z^2}\,\beta(\lambda_T,\lambda_R)\,\exp\left[-\int_0^z [\alpha(\lambda_T, z') + \alpha(\lambda_R, z')]\,dz'\right] \quad (1)$$

where,

z is the altitude of the volume element from which the return signal is scattered,

λ_T is the wavelength of the laser light transmitted,

λ_R is the wavelength of the backscatter light received,

$E_L(\lambda_T)$ is the light energy per laser pulse transmitted at wavelength λ_T,

$\xi_L(\lambda_T)$ is the net optical efficiency at wavelength λ_T of all devices (lenses, mirrors, etc.) in the optical path of the transmitter subsystem,

$\xi_R(\lambda_R)$ is the net optical efficiency at wavelength λ_R of all devices (lenses, mirrors, etc.) in the optical path of the receiver subsystem and detector subsystem,

c is the speed of light in air,

τ is time duration of the laser pulse,

A is the area of the receiving telescope aperture,

$\beta(\lambda_T,\lambda_R)$ is the back scattering cross section of the volume scattering element for the laser wavelength λ_T at Raman shifted wavelength λ_R,

$\alpha(\lambda_X,z')$ is the extinction coefficient at wavelength λ_X at range z'.

Upon examination of the equation, it becomes apparent that the Raman techniques that use the ratio of the signals at two wavelengths will greatly simplify the measurements of various parameters.

2.2. Water Vapor Measurements

The water vapor specific humidity, or mixing ration, are determined by taking the ratio of the signals from the 1st Stokes vibrational Raman shifts for water vapor and nitrogen. The measurement is made with laser transmission at visible (532 nm) and ultraviolet (266 nm) wavelengths. The visible measurement (660/607) is available at night and the ultraviolet measurement (294/284) is available day and night. The ultraviolet measurement is limited to the first 3 km of the atmosphere because of signal loss due to the large scattering cross-section. The specific humidity is determined from the relationship,

$$W(z) = K \frac{S_{H2O}(z)}{S_{N2}} \tag{2}$$

where the calibration factor, K, is verified by comparison with a rawinsonde balloon measurement when the instrument is moved to a new site. The ultraviolet wavelength value has remained relatively constant during the past three years, however the visible sensitivity has shown significant changes when the light level was sufficient to overload the photomultiplier tube. Investigation of the stability of the instrument has shown that the variation between the meteorological balloon sonde water vapor and the lidar is about ±4%, and this is approximately the value expected due to the spatial and temporal differences between the measuring techniques.[14]

2.3. Ozone Measurements

The Raman vibrational 1st Stokes shifts from molecular nitrogen and oxygen are used as the sources for ozone absorption measurement. Since the ratio of these two principal molecular constituents is constant to within 10 ppm in the lower atmosphere, any variation in the vertical profile of this ratio can be associated with the integrated absorption due to ozone. The only other species that has been found to be of concern at these wavelengths is SO_2, which we have observed in diesel exhaust plumes.[14,15] Table 2.1 shows the Raman energy, cross section and wavelength shift for nitrogen and oxygen when excited by 266 nm laser energy at the 4th harmonic of a Nd:YAG laser transmitter. Figure 2 shows the location of the Raman shifted wavelengths on the sloped side of the Hartley Band. Using a lidar inversion analysis technique, the quantity of ozone can be calculated.[8] This technique eliminates the difficult task of tuning and stabilizing the frequency and relative power of the transmitted wavelengths as required for DIAL measurements. The fact that the nitrogen and oxygen molecules scatter a known fraction of the two Raman wavelengths in each volume element makes the technique very robust against errors in the measurement.

Table 1. Atmospheric nitrogen and oxygen Raman Stokes energy and cross-section.[16]

	Vibrational Raman Energy	Cross Section	Wavelength Shift @ 266 nm
Nitrogen	2330.7 cm^{-1}	9.03 x 10^{-30} cm^2 sr^{-1}	284 nm
Oxygen	1556 cm^{-1}	11.86 x 10^{-30} cm^2 sr	278 nm

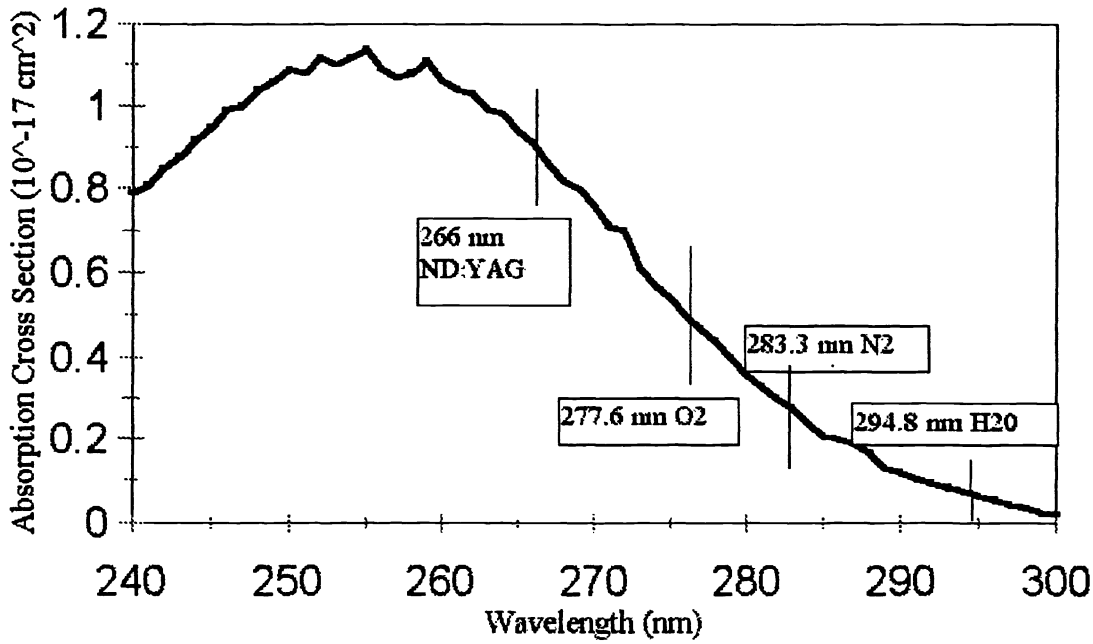

Figure 2. The absorption cross-section of the Hartley band of ozone is shown with the incident and scattered wavelengths indicated.[17]

The ozone profile is determined from the ratio of the return signal from the first Stokes Raman shifted scatter of nitrogen and oxygen molecules in the scattering volume,

$$\frac{P_{O2}(z)}{P_{N2}(z)} = \frac{\xi_R(\lambda_{O2})}{\xi_R(\lambda_{N2})} \frac{\beta(\lambda_L,\lambda_{O2},z)}{\beta(\lambda_L,\lambda_{N2},z)} \frac{\exp\left[-\int_0^z [\alpha(\lambda_{O2}, z')]\, dz'\right]}{\exp\left[-\int_0^z [\alpha(\lambda_{N2}, z')]\, dz'\right]} \tag{3}$$

To simplify the calculation, a system constant is chosen,

$$k_{system} = \frac{\xi_R(\lambda_{O2})}{\xi_R(\lambda_{N2})} \frac{\beta(\lambda_T,\lambda_{O2},z)}{\beta(\lambda_T,\lambda_{N2},z)} = \frac{\xi_R(\lambda_{O2})}{\xi_R(\lambda_{N2})} \frac{\sigma_{O2}}{\sigma_{N2}} \frac{[O_2]}{[N_2]} \tag{4}$$

where,

σ_{O2} is the Raman cross-section of oxygen at the laser wavelength,

σ_{N2} is the Raman cross-section of nitrogen at the laser wavelength,

$[O_2]$ is the concentration of oxygen in the atmosphere,

$[N_2]$ is the concentration of nitrogen in the atmosphere.

This constant is independent of altitude and has been calculated experimentally for the LAPS lidar system. The extinction coefficient is assumed to be equal to the sum of the absorption due to ozone, the scattering due to aerosols along the path and the scattering due to molecules;

$$\frac{\exp\left[-\int_0^z[\alpha(\lambda_{O2}, z')]\,dz'\right]}{\exp\left[-\int_0^z[\alpha(\lambda_{N2}, z')]\,dz'\right]} = \frac{\exp\left[-\int_0^z[\alpha_m(\lambda_{O2}, z')]\,dz'\right]}{\exp\left[-\int_0^z[\alpha_m(\lambda_{N2}, z')]\,dz'\right]} + \exp\left[-\int_0^z[\alpha_{O3}(\lambda_{O2}, z') - \alpha_{O3}(\lambda_{N2}, z') + \alpha_a(\lambda_{O2}, z') - \alpha_a(\lambda_{N2}, z')]\,dz'\right] \quad (5)$$

where:

$\alpha_{O3}(\lambda_x,z)$ is the attenuation due to absorption of ozone at wavelength λ_x,

$\alpha_a(\lambda_x,z)$ is the attenuation due to scattering and absorption of aerosols at wavelength λ_x,

$\alpha_m(\lambda_x,z)$ is the attenuation due to molecular scattering at wavelength λ_x.

The ozone absorption of a wavelength to be equal to the number of molecules, $N_{O3}(z)$, times the absorption cross-section, $\sigma_{O3}(\lambda)$, at a particular wavelength,

$$\alpha_{O3}(\lambda, z') = N_{O3}(z) \times \sigma_{O3}(\lambda)\ . \quad (6)$$

The number of ozone molecules can then be calculated from the relationship,

$$N_{O3}(z) = \frac{1}{\sigma_{O3}(\lambda_{O2}) - \sigma_{O3}(\lambda_{N2})} \frac{d}{dz}\left[\frac{P_{O2}(z)}{P_{N2}(z)} \frac{\exp\left[\int_0^z[\alpha_m(\lambda_{O2}, z')]\,dz'\right]}{\exp\left[\int_0^z[\alpha_m(\lambda_{N2}, z')]\,dz'\right]} \frac{1}{k_{system}}\right] - \frac{\alpha_a(\lambda_{O2}, z') - \alpha_a(\lambda_{N2}, z')}{\sigma_{O3}(\lambda_{O2}) - \sigma_{O3}(\lambda_{N2})} \quad (7)$$

2.4. Optical Extinction Measurements

The extinction coefficient is made up of components due to absorption by chemical species and particles, and scattering by molecules and particles. The molecular profiles from the Raman scatter signals provide direct measurements of the optical extinction. The signal at the transmitted wavelength exhibits a profile that combines molecular and particle scattering, and it is difficult to analyze for significant properties, except cloud height. However, analysis of the Raman profiles from molecular scattering signals can provide unique vertical profiles of optical extinction. The LAPS instrument measures the optical extinction profiles from the gradients in each of the measured molecular profiles, at 607, 530 and 284 nm. The wavelength dependent optical extinction can be used to describe changes in the particle size distribution as a function of altitude for the important small size particles. These measurements can then be interpreted to determine the air mass parameter and atmospheric optical density. Measurements of optical extinction are based upon gradients in the molecular profiles, using the N_2 vibrational Raman scattering or a band of the rotational Raman lines. The calculation is easily applied to the rotational Raman signal at 530 nm because it is so close to the 532 nm transmitted wavelength that no wavelength dependence exists. By first calculating the extinction at 532 nm from the 530 nm path, it is possible to then calculate the optical extinction at 607 nm without assuming any wavelength dependance.

The Raman lidar equation in the following form indicates the important elements contributing to extinction,

$$P_R(z) = \frac{\xi(z)}{z^2} N(z) \frac{\partial\sigma}{\partial\Omega} \exp\left(-\int^z(\alpha_{O,\,mol} + \alpha_{R,\,mol} + \alpha_{O,\,aer} + \alpha_{R,\,aer})dz\right) \quad (8)$$

where, O = outgoing wavelength, 532 or 266 nm, and R = return wavelength, 530 (rot), 607 (N_2), 284 (N_2) or 278 (O_2) nm.

$$\alpha_{R,\,aer} = \frac{d}{dz}\left[\ln \frac{N(z)}{P_R(z)\cdot z^2}\right] - \alpha_{O,\,mol}(z) - \alpha_{R,\,mol}(z) - \alpha_{O,\,aer}(z)$$

$$\alpha_{530,\,aer} = \frac{d}{dz}\left[\frac{1}{2}\ln \frac{N(z)}{P_{530}(z)\cdot z^2}\right] - \alpha_{532,\,mol}(z) \tag{9}$$

The difference in the absorption of aerosol at the two wavelengths is generally small and can be neglected. The molecular scattering in this equation is calculated using the standard profile of the atmosphere given the pressure, temperature, and humidity at ground level,

$$\exp\left[\int_0^z [\alpha_{molecular}(\lambda, z')]\, dz'\right] = \exp\left[\int_0^z [N * H * (1 - \exp\left(\frac{-z'}{H}\right) * S]\, dz'\right] \tag{10}$$

where:

N is the number density at ground level

H is the scale height H = kT/(mg)

S is the Rayleigh scattering cross section.

3. LAPS INSTRUMENT

The LAPS lidar instrument has been developed from lessons learned during the development and testing of five prior lidar research instruments. The LAPS instrument was fabricated during FY95/96 and was deployed onboard the USNS Sumner, a Navy survey ship, in the Gulf of Mexico and along the Atlantic coast of Florida during September-October 1996, to perform tests and validate its performance.[14,18] The LAPS instrument was designed to provide the real-time data product of meteorological properties and RF-refractive conditions with automated control of most operating features. Several sub-systems have been designed into the instrument to control and simplify the instrument operation. It is intended that a weather officer could obtain the data on demand or acquire data according to some planned schedule. The long term goal for this instrument development is to replace most of the current balloon sonde profiling and thus enable data collection at more frequent intervals to support operations and requirements for meteorological data.

The shipboard testing of the Lidar Atmospheric Profile Sensor (LAPS) instrument was intended to demonstrate its ability to measure the atmospheric properties and demonstrate the capability for automated operation under a wide range of meteorological conditions. The instrument measures the water vapor profile based on the vibrational Raman scattering, and the temperature profile based on the rotational Raman scattering. These measurements provide real-time profiles of RF refractivity. Profiles are currently obtained at each minute, with a vertical resolution of 75 meters from the surface to 7 km. The vertical resolution will be improved to the range of 3 to 15 meters using a new fast electronics package, which has recently been demonstrated in our laboratory. The LAPS instrument includes several sub-systems to automate the operation and provide the real-time profiles. Also, the instrument includes an X-band radar which detects aircraft as they approach the beam and automatically protects a 6 degree cone angle around the beam. The instrument also includes self-calibration and built-in-tests to check many functions. Table 2 lists the primary characteristics of the LAPS lidar and Table 3 lists the measurements obtained and the typical altitude range of the data products expected.

Table 2. LAPS Lidar characteristics

Transmitter	Continuum 9030 -- 30 Hz 5X Beam Expander	600 mj @ 532 nm 130 mj @ 266 nm
Receiver	61 cm Diameter Telescope	Fiber optic transfer
Detector	Seven PMT channels Photon Counting	528 and 530 nm -- Temperature 660 and 607 nm -- Water Vapor 294 and 285 nm -- Daytime Water Vapor 276 and 285 nm -- Raman/DIAL Ozone
Data System	DSP 100 MHZ	75 meter range bins
Safety Radar	Marine R-70 X-Band	protects 6° cone angle around beam

Table 3. Measurements made by the LAPS lidar instrument

Property	Measurement	Altitude	Time Resolution
Water Vapor	660/607 Raman 294/285 Raman	Surface to 5 km Surface to 3 km	Night - 1 min. Day & Night - 1 min.
Temperature	528/530 Rotational Raman	Surface to 5 km	Night 30 min.
Ozone	276/285 Raman/DIAL	Surface to between 2 and 3 km	Day and Night 30 min.
Optical Extinction at 530 nm	530 nm Rotational Raman	Surface to 5 km	Night 10 to 30 min.
Optical Extinction at 607 nm	607 N_2 1st Stokes	Surface to 5 km	Night 10 to 30 min.
Optical Extinction at 285 nm	285 N_2 1st Stokes	Surface to 3 km	Day and Night 30 min.

4. RESULTS AND EXAMPLES OF APPLICATIONS TO AIR QUALITY

The LAPS instrument uses Raman lidar techniques to simultaneously provide the profiles of water vapor, temperature, ozone and optical extinction. The goal of this paper is to introduce the measurements using examples from the recent application of the techniques to investigations of air quality. The results presented here were obtained during measurements of a research program referred to as the North American Research Strategy for Tropospheric Ozone - Northeast - Oxidant and Particle Study (NARSTO-NE-OPS).[19] The program is conducted by a consortium of universities and government laboratories and its focus is on the urban corridor extending through the northeastern states. The primary measurement site is located in Philadelphia, PA. Figure 3 shows examples of profiles of water vapor, ozone and optical extinction. The water vapor profiles obtained with the LAPS instrument are shown together with measurements from a tethersonde of Millersville University (Richard Clark) and aircraft measurements form the University of Maryland (Bruce Doddridge). These daytime measurements show the variations of an active convective boundary layer. The ozone profiles of the LAPS instrument and the University of Maryland aircraft are compared at night when the ozone profile is almost constant in the region of the residual boundary layer between 200 and 1700

meters. In the free troposphere, ozone patches can exist for relatively long period of time and are frequently observed to drift in the background wind, as observed in this case. Within the thin nocturnal boundary layer, below 200 meters, the ozone is lost due to deposition and oxidation at the surface as well as loss from surface layer chemical processes. The optical extinction profiles are shown for wavelengths at visible and ultraviolet wavelengths. It is interesting to note that the visible wavelengths exhibit a strong correlation with water vapor content of the atmosphere, as would be expected for the hygroscopic sulfate and nitrate aerosols that are the dominate types in the eastern states. However the ultraviolet extinction profile, which could represent slightly smaller particles, does not appear to correlate with the water vapor content and could represent the carbonaceous or volatile organic materials that are non-hygroscopic. The temperature profiles are not represented here but they are less meaningful for interpretation of air quality issues. Profiles such as these can be useful at specific times, however, the time sequence of the properties is much more useful in understanding the physical and chemical processes.

The results shown in Figure 4 are taken from the time period of the major air pollution episode that occurred in the region during the summer of 1998. The measurements of the profiles of water vapor, ozone and optical extinction at 284 nm are shown for a 24 hour period. The water vapor results are shown at 1 minute time steps with 5 minute smoothing. These results show the convective plumes as they move past the vertical beam of the lidar. At 1700 UTC (1 PM local time), the elevated layer meets and mixes with the rising boundary layer. Back trajectories of the air mass show that it originated in the mid-west industrialized region. The ozone and optical extinction measurements show interesting response to the arrival of the air mass at 1700 UTC. Based upon the apparent initiation of the air pollution event being coincident with the arrival of the air mass, we have postulated that it contained precursor chemicals that triggered the pollution episode. During the nighttime period shown near the middle of the second panel, the background wind began to dissipate and redistribute the ozone and particulate matter.

5. CONCLUSIONS

Measurements of the variations in the profiles of optical extinction, water vapor, and ozone provide valuable insight into the evolution of pollution events. Data taken on 21 August showed a sudden increase of ozone in the planetary boundary layer when a plume, which had been transported aloft in an elevated layer from the Midwest region, was mixed into the PBL. Since low ozone levels were observed at the surface before the plume arrived and little ozone was observed inside the plume, it was determined that this rise was due to the presence of ozone precursors transported inside the plume. The water vapor profiles show the exact timing of the pollution event, which occurred when the thickening boundary layer mixed the plume material to the surface. These measurements show, for the first time, a sequence of dynamical processes occurring in the lower atmosphere that demonstrate the importance of vertical mixing, horizontal transport, and storage of precursor materials in an elevated layer. The details revealed in the time sequences of the lidar data add a new dimension to understand the evolution of air pollution episodes. The vertical profile information and temporal variations are expected to provide the critical tests for the models under development that are expected to be the basis for future policy development. The continuous vertical profiles that can be obtained using lidar provide an important dimension for investigating the physical and chemical process of the atmosphere.

6. ACKNOWLEDGMENTS

Air quality investigations discussed are supported by the US EPA grant entitled "Investigations of Factors Determining the Occurrence of Ozone and Fine Particles in Northeastern USA," grant number R826373. The PSU lidar development, shipboard testing, and evaluation at several field sites have been supported by the US Navy through SPAWAR Systems Division - San Diego, PMW-185, NAVOCEANO, NAWC Point Mugu, ONR, DOE, EPA, CARB, NASA and NSF. The hardware and software development has been possible because of the excellent engineering and technical efforts of several engineers and technicians at the PSU Applied Research Laboratory and the graduate students of the Department of Electrical Engineering. Special appreciation goes to D.B. Lysak, T.M. Petach, T.D. Stevens, P.A.T. Haris, M. O'Brien, and S.T. Esposito.

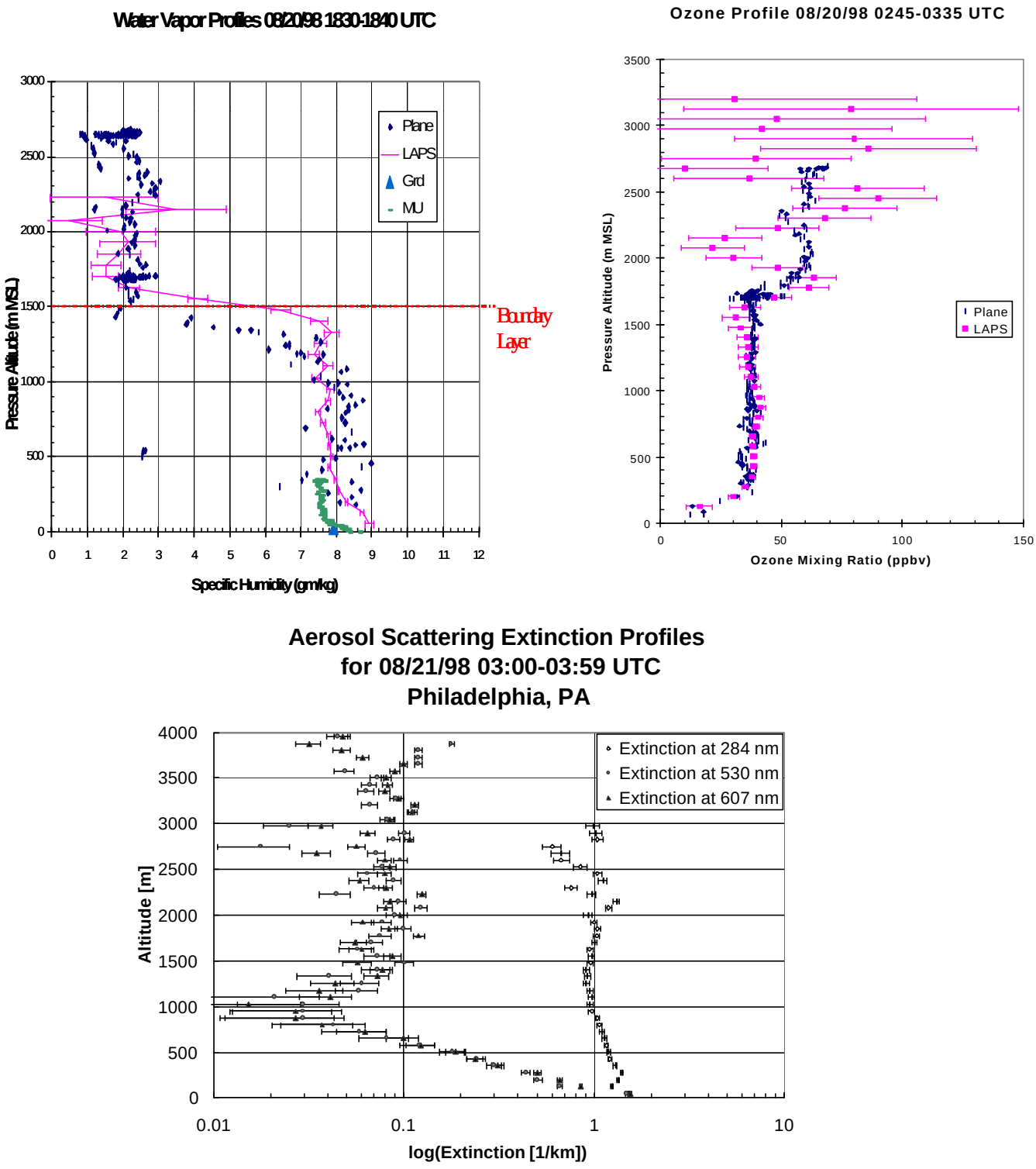

Figure 3. Examples of three sets of profiles measured by the LAPS lidar as part of the NARSTO-NE-OPS program in Philadelphia during August 1998. The water vapor measurements from LAPS lidar, the Millersville University tether sonde, and University of Maryland aircraft are compared. An ozone profile of the LAPS lidar is compared with the University of Maryland aircraft. The LAPS optical extinction profiles at visible and ultraviolet wavelengths are compared.

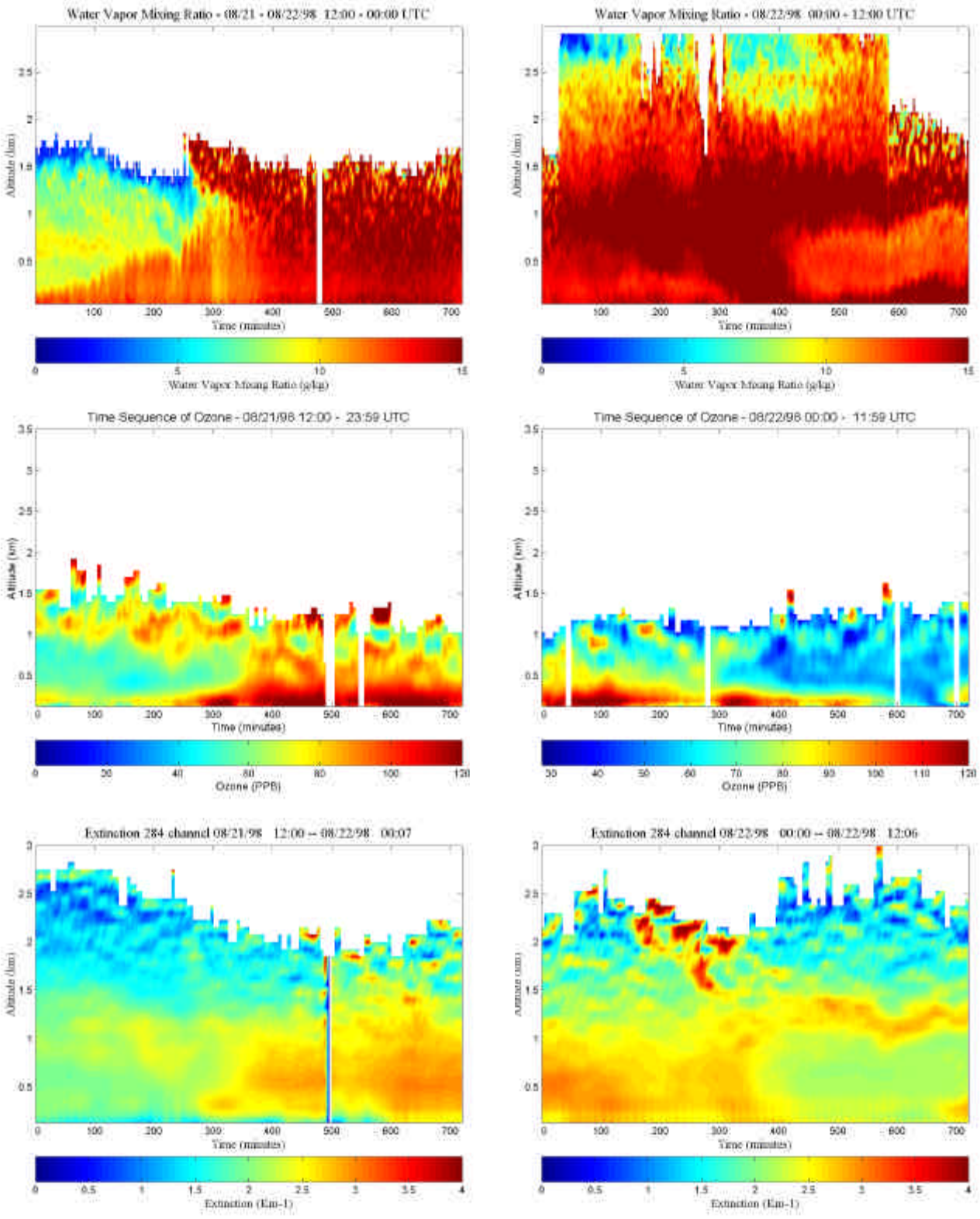

Figure 4. A set of 24 hour time sequences, which depict the water vapor, ozone and optical extinction are shown for the period from 12 hours UTC on 21 August to 12 hours UTC on 22 August 1998, capture some interesting features of an air pollution episode. An elevated layer, which is observed to mix with the rising boundary layer at 17 UTC (1 PM local), appears to trigger an air pollution event which results in high concentrations of ozone and airborne particulate matter.

7. REFERENCES

1. Mauderly, Joe, Lucas Neas, and Richard Schlesinger, "PM Monitoring Needs Related to Health Effects", *Proceedings of the PM Measurements Research Workshop*, EPA Report No. 2, Chapel Hill, North Carolina, pp 9-14, July 22-23, 1998.

2. Albritton, Daniel L., and Daniel S. Greenbaum, "Atmospheric Observations: Helping Build the Scientific Basis for Decisions Related to Airborne Particle Matter", *Proceedings of the PM Measurements Research Workshop*, EPA Report No. 1, Chapel Hill, North Carolina, pp. 1-8, July 22-23, 1998.

3. Hidy, G. M., P. M. Roth, J. M. Hales and R. Scheffe, "Oxidant Pollution And Fine Particles: Issues And Needs," NARSTO Critical Review Series, 1998, http://odysseus.owt.com/Narsto/

4. Philbrick, C.R., "Raman Lidar Measurements of Atmospheric Properties", *Atmospheric Propagation and Remote Sensing III*, SPIE Vol. 2222, 922-931, 1994.

5. Balsiger, F., and C. R. Philbrick, "Comparison of Lidar Water Vapor Measurements Using Raman Scatter at 266nm and 532 nm," in *Applications of Lidar to Current Atmos. Topics*, SPIE Proc. Vol. 2833, 231-240 1996.

6. Balsiger, F., P. A. T. Haris and C. R. Philbrick, "Lower-tropospheric Temperature Measurements Using a Rotational Raman Lidar," in *Optical Instruments for Weather Forecasting*, SPIE Proc. Vol. 2832, 53-60, 1996.

7. Haris, P.A.T., "Pure Rotational Raman Lidar for Temperature Measurements in the Lower Troposphere," PhD Thesis for Penn State University, Department of Electrical Engineering, August 1995.

8. Esposito, S.T., and C.R. Philbrick,"Raman/DIAL Technique for Ozone Measurements," *Proceeding of Nineteenth International Laser Radar Conference*, NASA/CP-1998-207671/PT1, pp 407-410, 1998.

9. Philbrick, C.R., "Raman Lidar Capability to Measure Tropospheric Properties," *Proceeding of Nineteenth International Laser Radar Conference*, NASA/CP-1998-207671/PT1, pp 289-292, 1998.

10. O'Brien, M.D., T. D. Stevens and C. R. Philbrick, "Optical Extinction from Raman Lidar Measurements," in *Optical Instruments for Weather Forecasting*, SPIE Proceedings Vol. 2832, 45-52, 1996.

11. Philbrick, C.R., M. D. O'Brien, D, B. Lysak, T. D. Stevens and F. Balsiger, "Remote Sensing by Active and Passive Optical Techniques," *NATO/AGARD Proceedings on Remote Sensing*, AGARD-CP-582, 8.1-8.9, 1996.

12. Philbrick, C.R., D.B. Lysak, Jr., M. O'Brien and D.E. Harrison, "Lidar Measurements of Atmospheric Properties," in *Proceedings of the Electromagnetic/Electro-Optics Performance Prediction and Products Symposium*, Naval Post Graduate School, Monterey CA, 385-400, June 1997.

13. Philbrick, C.R., and D.B. Lysak, Jr., "Atmospheric Optical Extinction Measured by Lidar," *Proceedings of the NATO-SET Panel Meeting on E-O Propagation*, NATO RTO-MP-1, pp.40-1 to 40-7, 1998.

14. Philbrick. C.R., and D. B. Lysak, Jr., "Optical Remote Sensing of Atmospheric Properties," *Proceedings of the Battlespace Atmospheric and Cloud Impacts on Military Operations (BACIMO)*, Air Force Research Laboratory, AFRL-VS-HA-TR-98-0103, pg 460-468, 1999.

15. Sedlacek, III, A.J., M.D. Ray and M. Wu, "Augmenting Classical DIAL with Raman-DIAL (RaDIAL)," in *Application of Lidar to Current Atmospheric Topics III*, SPIE Proc. Vol.3757, 126-139, 1999.

16. Measures, Raymond M., Laser Remote Sensing.Wiley-Interscience, New York: 1984.

17. Inn, E.C., and Y. Tanaka, "Absorption Coefficient of Ozone in the Ultraviolet and Visible Regions," J. *Optical Society*, 43, 870-873, 1953.

18. Philbrick, C.R., and D. B. Lysak, Jr., "Lidar Measurements of Meteorological Properties and Profiles of RF Refractivity," *Proceedings of the 1996 Battlespace Atmospherics Conference*, Technical Document 2938 NCCOSC RDT&E, pg 595-609, 1996.

19. Philbrick, C.R., "Investigations of Factors Determining the Occurrence of Ozone and Fine Particles in Northeastern USA," *Proceedings of Symposium on Measurement of Toxic and Related Air Pollutants*, Air &Waste Management Association, pp 248-260, 1998.